Running title: Functional proteomics of human breast tumors

Title: A novel approach to the study of the functional proteome in breast cancer

Running title: Functional proteomics of human breast tumors

Bryan Hennessy[1,2,3*], Yiling Lu[4*], Ana Maria Gonzalez-Angulo[3,4,5], Mark Carey[4], Simen Myhre[6,7], Zhenlin Ju[8], Kevin Coombes[8], Funda Meric-Bernstam[9], Isabelle Bedrosian[9], Michael A. Davies[10], Doris Siwak[4], Roshan Agarwal[4], Fan Zhang[4], Jens Overgaard[11], Jan Alsner[11], Richard M Neve[12], Wen-Lin Kuo[12], Joe W Gray[12], Anne-Lise Borresen-Dale[6,13], Gordon B Mills[3,4]

* Drs Hennessy and Lu contributed equally to this work.

1. Corresponding author (Telephone 7135631792; Fax 7135451541; Email bhennessy@mdanderson.org)

2. Department of Gynecologic Medical Oncology, The University of Texas M. D. Anderson Cancer (MDACC), 1515 Holcombe Blvd., Houston, TX 77030, USA

3. Kleberg Center for Molecular Markers, MDACC

4. Department of Systems Biology, MDACC

5. Department of Breast Medical Oncology, MDACC

6. Department of Genetics, Institute for Cancer Research, Norwegian Radium Hospital, Rikshospitalet University Hospital, Oslo, Norway

7. Faculty division, The Norwegian Radium Hospital, Faculty of Medicine, University of Oslo, Norway.

8. Department of Bioinformatics and Computational Biology, MDACC

9. Department of Surgical Oncology, MDACC

10. Department of Melanoma Medical Oncology, MDACC

11. Department of Experimental Clinical Oncology, Aarhus University Hospital, Aarhus, Denmark

12. Lawrence Berkeley National Laboratory, Berkeley, CA

This work was supported in part by the Kleberg Center for Molecular Markers at M. D. Anderson Cancer Center, by NCI PO1CA099031 (to G.B.M.), by The Susan G. Komen Foundation Biomarkers Identification and Validation Award FAS0703849 (to B. T. H., A. M. G., G. B. M.) and by the Research Council of Norway grant 175240/S10 (to A.L.B.-D.). Work was also supported by the U.S. Department of Energy under Contract No. DE-AC02-05CH1123.

Conflicts of Interest: None

Running title: Functional proteomics of human breast tumors

Abbreviations

AcCoA: acetyl coenzyme A carboxylase

AcCoAp: phosphorylated acetyl coenzyme A carboxylase at serine 79

AMP: adenosine monophosphate

AMPK: AMP activated protein kinase

AMPKp: phosphorylated AMP activated protein kinase at serine 172

ANOVA: analysis of variance

BCA: bicinchoninic acid

CCNB1: cyclin B1

CCND1: cyclin D1

CCNE1: cyclin E1

CMF: cyclophosphamide, methotrexate and 5-fluorouracil chemotherapy

CV: coefficients of variation

DAB: diaminobenzidine

DFS: disease-free survival

EGF: epidermal growth factor

EGFR: epidermal growth factor receptor

ERα: estrogen receptor alpha

FC: fold change

FFPE: formalin fixed paraffin-embedded

FISH: fluorescent in situ hybridization

FT: frozen tumor

GSK3: glycogen synthase kinase 3

Running title: Functional proteomics of human breast tumors

HER2: human epidermal receptor 2

HR: hormone receptor

IRB: Institutional Review Board

IHC: immunohistochemistry

Log2: log to the base 2

MDACC: The University of Texas M. D. Anderson Cancer Center

mRNA: messenger ribonucleic acid

mTor: mammalian target of rapamycin

PI3K: phosphatidylinositol-3 kinase

PR: progesterone receptor

RPPA: reverse phase protein lysate array

S: serine

Stat3: signal transducer and activator of transcription

T: threonine

Y: tyrosine

Running title: Functional proteomics of human breast tumors

Summary

Factors including intratumoral heterogeneity and variability in tissue handling potentially hamper the application of reverse phase protein arrays (RPPA) to study of the solid tumor functional proteome. To address this, RPPA was applied to quantify protein expression and activation in 233 human breast tumors and 52 breast cancer cell lines. Eighty-two antibodies that recognize kinase and steroid signaling events and their effectors were validated for RPPA because of the importance of these proteins to breast carcinogenesis. Reproducibility in replicate lysates was excellent. Intratumoral protein expression was less variable than intertumoral expression, and prognostic biomarkers retained the ability to accurately predict patient outcomes when analyzed in different tumor sites. Although 21/82 total and phosphoproteins demonstrated time-dependent instability in breast tumors that were placed at room temperature after surgical excision for 24 hours prior to freezing, the functional proteomic 'fingerprint' was robust in most tumors until at least 24 hours before tissue freezing. Correlations between RPPA and immunohistochemistry were statistically significant for assessed proteins but RPPA demonstrated a superior dynamic range and detected, for example, an 866-fold difference in estrogen receptor alpha level across breast tumors. Protein and mRNA levels were concordant (at $p \leq 0.05$) for 41.3% and 61.1% of assayed targets in breast tumors and cell lines, respectively. Several phosphorylation and cleavage products did not correlate with the corresponding transcript levels. In conclusion, the reproducibility of RPPA, the faithfulness with which proteins and the functional proteomic 'fingerprint' are preserved in different sections derived from primary breast tumors, and the surprising stability of this 'fingerprint' with increasing time to freezing all facilitate the application of RPPA to the accurate study of protein biomarkers in non-microdissected tumor specimens. The lack of correlation between several protein phosphorylation and cleavage

products and the corresponding transcripts underlines the importance of study of the functional proteome in cancer.

Introduction

Much progress has been made in genomic breast cancer classification. [1-10] However, as mRNA levels do not translate precisely into protein function due to post-translational modifications, mRNA profiling cannot characterize the functional proteome. Proteins are the ultimate effectors of cellular outcomes. Thus, the lack of a validated, practical, moderate- to high-throughput, quantitative functional proteomics platform remains a key barrier to the identification and validation of solid tumor biomarkers.

Traditional protein assays including immunoblotting and immunohistochemistry (IHC) can assess only a small numbers of proteins, and are expensive, semiquantitative and require large amounts of material. Although mass spectroscopy is promising, it is not currently sufficiently robust or cost effective for clinical implementation.

Reverse phase protein lysate arrays (RPPA) offer an emerging approach to comprehensive quantitative profiling of the levels and function of multiple proteins in tumors.[11-18] By providing high-throughput, low-cost, objective analysis of multiple proteins in small amounts of sample, RPPA has the potential to map protein levels and function in intracellular pathways in a comprehensive, convenient, and sensitive manner.

Although RPPA is validated for in-vitro analyses[11-18], several questions remain to be resolved prior to its routine application to human breast tumors. RPPA does not provide information concerning spatial organization. Intratumoral heterogeneity in protein expression and activation thus poses a potential challenge to implementation. Variability in tissue handling may also result

in unpredictable changes in the expression and post-translational modification (e.g. phosphorylation) of proteins. The validation of a large panel of antibodies is required since RPPA is essentially a high-throughput 'dot-blot' and therefore is unable to distinguish between specific and off-target antibody-protein interactions. The goal of this study is to address obstacles to the successful application of RPPA to the study of solid tumors and in this case specifically the breast cancer functional proteome.

Experimental Proceedures

Antibodies and reagents

Eighty-two antibodies were used (**Supplemental Table 1**). These antibodies were chosen because of the importance of the detected proteins to breast carcinogenesis.[19-39] The AKT inhibitor perifosine was obtained from Keryx Pharmaceuticals (New York, NY). The phosphatidylinositol-3 kinase (PI3K) inhibitor LY294002 was obtained from Calbiochem (San Diego, CA). Rapamycin was obtained from Cell Signaling, Inc. (Danvers, MA). Epidermal growth factor (EGF) was purchased from R&D Systems, Inc. (Minneapolis, MN).

Cell lines and tumor samples

The MDAMB231, MDAMB468, MCF7, T47D, ZR75-1, OVCAR3 and SKOV3 cell lines were obtained from the American Type Culture Collection (Manassas, VA). The protein lysates of 52 breast cancer cell lines were obtained from Dr. Joe W. Gray. Ninety-five primary breast tumors were obtained from the breast tumor frozen tissue bank at M.D. Anderson Cancer Center (MDACC) under an Institutional Review Board (IRB)-approved protocol (Set A (**Supplemental Table 2**)). Protein was extracted from these 95 tumors, including from two independent sections derived from 49 tumors ('biologic replicates'). For comparison of RPPA with transcriptional profiling (protein-mRNA correlations), 128 primary breast tumors were obtained from patients

treated in the Danish DBCG82 b and c studies (PMID: 10335782)[40] (Set B (**Supplemental Table 2**)).

For the studies of intratumoral heterogeneity and total and phosphoprotein stability, a prospective study was undertaken to collect primary breast tissue at breast surgery in ten patients with breast cancer under an IRB-approved protocol. Each tumor was sectioned with assistance from a breast pathologist and immediately snap frozen (three pieces) or left at room temperature for 0.5/1/2/4/6/24 hours (1 piece/timepoint) prior to freezing (-85C). Protein was extracted from each piece of tumor without thawing.

Lysate preparation and array spotting

Breast cancer cell lines were cultured in their optimal medium with 5% fetal bovine serum in 6-well-plates. For experiments involving cell line treatment or stimulation, the cells were starved overnight and treated with inhibitor with or without epidermal growth factor (EGF) stimulation (20 ng/ml for 10 minutes). Cells were then washed twice with PBS and lysed in ice-cold lysis buffer (1% Triton X-100, 50mm HEPES, pH 7.4, 150mM NaCl, 1.5mM $MgCl_2$, 1mM EGTA, 100mM NaF, 10mM Na Pyrophosphate, 1mM Na_3VO_4, 10% glycerol) supplemented with proteinase inhibitors (Roche Applied Science, Indianapolis, IN). Cellular protein concentration was determined by bicinchoninic acid (BCA) reaction (Pierce, Rockford, IL). Frozen tumor tissue (≤10mg) was homogenized after macrodissection in lysis buffer at 40mg/ml by PowerGen polytron homogenizer (Fisher Scientific, Hampton, NH) and the concentration of the protein lysates corrected to 1.33 mg/mL. After centrifugation, post-nuclear detergent lysates (3 parts) were boiled with a solution (1 part) of 4XSDS (90%)/B mercapto-ethanol (10%). Five serial twofold dilutions were performed in lysis buffer containing 1% SDS (dilution buffer). The

diluted lysates were spotted on nitrocellulose-coated FAST slides (Whatman, Schleicher & Schuell BioScience, Inc., Keene, NH) by a robotic GeneTAC (Genomic Solutions, Inc., Ann Arbor, MI) G3 arrayer or an Aushon Biosystems (Burlington, MA) 2470 arrayer.

Antibody probing and signal detection of RPPA

The DAKO (Carpinteria, CA) catalyzed signal amplification system was used for antibody blotting. Each slide was incubated with a primary antibody (**Supplemental Table 1**) in the appropriate dilution. The signal was captured by biotin-conjugated secondary antibody and amplified by tyramide deposition. The analyte was detected by avidin-conjugated peroxidase reactive to its substrate chromogen diaminobenzidine (DAB). Subsequently, the slides were individually scanned, analyzed, and quantitated using MicroVigene software (VigeneTech Inc., North Billerica, MA). This software provides automated spot identification, background correction and individual spot intensity determination (expressed in logarithmic units).

Immunoblotting

Lysates were prepared as described above. Proteins were resolved in SDS PAGE and transferred to PVDF membranes. The membranes were blocked by 5% BSA and hybridized with different primary antibodies as indicated. Signals were captured by Horse Radish Peroxidase-conjugated secondary antibody and visualized by the enhanced chemiluminescence system (Amersham Pharmacia Biotech, Piscataway, NJ). The abundance of immunoreactive protein was quantified using a computing densitometer (NIH Imaging) and presented as arbitrary units of density.

Transcriptional profiling

Expression data for Set B (**Supplemental Table 2**) were generated at Norwegian Radium Hospital. The microarray system used was the Applied Biosystems Human Genome Survey Microarray version 2.0. These are whole genome arrays spotted with 32878 probes covering

29098 genes. The platform utilizes chemiluminescence labeling in a single channel system. Details can be found at the following website: http://www3.appliedbiosystems.com/cms/groups/mcb_marketing/documents/generaldocuments/cms_040420.pdf

Statistical analysis

R and NCSS (Kaysville, Utah) softwares were used. The spot signal intensity data from MicroVigene are processed by the R package SuperCurve (version 1.01)[18], available at "http://bioinformatics.mdanderson.org/OOMPA". A fitted curve (called "supercurve") is plotted with the signal intensities on the Y-axis and the relative log2 concentration of each protein on the X-axis using the non-parametric, monotone increasing B-spline model (**Figure 1**).[18] The protein concentrations are derived from supercurve for each sample lysate on the slide by curve-fitting and then normalized by median polish. Each total and phosphoprotein measurement is subsequently corrected for loading using the average expression of all measured proteins. For the study of total and phosphoprotein stability, the expression of each protein in the three immediately frozen replicate sections of 10 primary breast tumors was averaged, measurements at six later time points (0.5/1/2/4/6/24 hours) were treated as separate observations, and the effects of time to freezing on total and phosphoprotein expression were tested using an analysis of variance (ANOVA) model. The effects of intratumoral and intertumoral variability on protein expression were tested by applying ANOVA models to RPPA data derived from the three immediately frozen replicate sections of 10 breast tumors. To estimate disease-free survival (DFS), the time to breast cancer relapse or death (whichever came first) since diagnosis was computed. DFS time was censored at last follow up if neither relapse nor death occurred. DFS probabilities were estimated using Kaplan-Meier's product limit method.

Results

Antibody validation

Antibody validation for RPPA is critical to ensure that the detected signal is predominantly representative of the protein of interest. We chose 82 antibodies that recognize kinase and steroid signaling events and their effectors (**Supplemental Table 1**) because of the importance of these proteins to breast carcinogenesis.[19-37] The relative protein levels derived from RPPA[18] are correlated with the density of the appropriately sized band on immunoblots of the corresponding protein lysates. An arbitrary correlation coefficient (R) of ≥0.7 is required for each antibody (**Figure 1A**). Antibodies that 'see' multiple 'off-target' western blot bands or a dominant non-specific band are not suitable for RPPA, and an alternative antibody is sought. For phospho-specific (p) antibodies, cell lines are manipulated in a fashion (e.g. with inhibitors and growth factors) that will alter the phosphorylation site to ensure that observed signal changes are correlated between immunoblotting and RPPA (**Figure 1B**). For proteins whose expression does not demonstrate a sufficient dynamic range to facilitate antibody validation, siRNA is used to manipulate the signal to allow evaluation of RPPA-immunoblotting correlations. Further, protein and mRNA levels are compared (**Supplemental Table 3**); when levels are concordant, as they are with 41.3% of assayed targets in human breast tumors (at $p \leq 0.05$), this provides additional confidence in the validity of RPPA. Using these approaches, we continue to expand the antibody list with particular emphasis on important proteins in breast carcinogenesis**.** A web site will be made available with publication of this manuscript with demonstration of the utility of all antibodies in the format shown in Figure 1 (http://10.106.178.152:8080/AntibodyDatabase/index.html).

Reproducibility

Using four antibodies as examples, reproducibility was excellent when the same lysates were printed on the same slides and on different slides for protein quantification using RPPA (**Supplemental Figure 1/Figure 2**), with coefficients of variation (CVs) that were consistently <15%.

Total and phosphoprotein stability

A major challenge to the study of patient tumors is the potential that protein levels and particularly post-translational modifications will change between the time of tissue collection and analysis. However, as RPPA is a "dot-blot" approach, it may be less susceptible to proteolysis than immunoblotting. To evaluate total and phosphoprotein stability, ten human breast tumors were obtained at surgery, processed and analyzed by RPPA (see Methods). **Supplemental Folder 1** shows **t**he time plots for all 82 total and phosphoproteins. Strikingly, the levels of 61/82 proteins including several phosphoproteins were stable up to 24 hours after tumor collection before freezing (**Figure 3/Supplemental Figure 2/Table 1**). Thus, although breast tumors must be frozen as soon as possible after excision to preserve the integrity of our ability to assess all signaling events, many total and phosphoprotein levels do not change markedly over time, allowing analysis in samples that have not been rapidly frozen.

Intra- versus intertumoral heterogeneity in protein and phosphoprotein expression

The effects of intratumoral and intertumoral variability on protein and phosphoprotein expression were tested by applying ANOVA models to RPPA data derived from 10 breast tumors. Of 82 proteins in three time 0 breast tumor replicates, 80 demonstrated significant variability across the ten tumors, while the expression of only 8 total and phosphoproteins demonstrated significant intratumoral variability (**Supplemental Table 4**). **Supplemental Folder 2/ Supplemental Table 4** demonstrate at time 0 the maximum intertumoral fold change

(FC) and the individual and mean intratumoral FCs for each antibody in log2 units. Overall, intratumoral total and phosphoprotein levels are much less variable than intertumoral levels, a technical and biologic necessity for robust identification of biomarkers. Therefore, the collection of biologic replicates of individual tumors that are snap frozen after excision may not be necessary for accurate and reproducible analysis of protein expression and function by RPPA.

Intratumoral heterogeneity and the robustness of functional proteomic biomarkers

To determine the impact of intratumoral heterogeneity on the robustness and reproducibility of functional proteomic biomarkers, we firstly determined the correlation coefficients between protein expression levels in protein lysates derived from each of two separate sections ('biologic replicates') obtained from 49 primary hormone receptor-positive breast tumors **(Supplemental Table 5)**. These correlation coefficients were not as high as those associated with replicate protein lysates derived from the same tumor sections ('technical replicates') likely due in part to the modest degree of intratumoral heterogeneity described above. However, most correlation coefficients (72%) between 'biologic replicates' were statistically significant ($p<0.001$).

Next, the total and phosphoproteins associated with differential disease-free survival (DFS) times were determined in each cohort of 49 'biologic replicates.' High expression of p53 and cyclin B1, which both showed minimal intratumoral variability, were significantly associated with short DFS times in both cohorts (**Figure 4**), while, low levels of phospho-MAPK (Thr202/Tyr204) were significantly associated with short DFS in both cohorts (not shown). In both cohorts, low levels of estrogen (ERα) and progesterone receptors (PR) and low phosphorylation of stat3 at Ser727 were associated with a trend ($p=0.05$-0.1) to shorter DFS times.

An integrated analysis of multiple proteins may facilitate more accurate prediction of clinical endpoints than analysis of individual proteins. Thus, we next determined if the expression and activation levels of multiple proteins yield a stable functional proteomic 'fingerprint' despite intratumoral heterogeneity and variability in tumor handling prior to freezing. Using the ten breast tumors obtained at surgery, on unsupervised clustering, the 82-protein functional proteomic 'fingerprint' was faithfully preserved across three snap frozen (time 0) sections derived from nine of the 10 tumors (**Figure 5A**). Further, this 'fingerprint' was faithfully preserved in most tumors with increasing time to tumor freezing up to 24 hours after resection (**Figure 5B**). In two cohorts of separate sections derived from each of 49 breast tumors, the functional proteomic signatures associated with each corresponding pair of sections was significantly correlated in 43 tumors (**Supplemental Figure 3**). Overall, in terms of intratumoral heterogeneity, the data suggest that the quantification of total and phosphoproteins by RPPA in primary breast tumors is reproducible in snap frozen tissue without microdissection. Although the expression of 21/82 total and phosphoproteins was significantly affected by time to tumor freezing, the functional proteomic 'fingerprint' is reproducible in most tumors even after a delay of 24 hours before freezing.

Correlations between RPPA and IHC

In 95 breast tumors (Set A (**Supplemental Table 2**)), the levels of ERα and PR proteins, respectively, determined by RPPA were significantly higher in tumors that are categorized by IHC and fluorescent in situ hybridization (FISH) as hormone receptor-positive compared with levels in triple receptor-negative ($p=0.00004$, <0.001) and HER2-amplified breast cancers ($p=0.01$, <0.001). There were significant positive correlations between ERα and PR levels determined by RPPA and the percentage positivity of these proteins as assessed using IHC

(p=0.002, 0.0006, respectively). Among 64 hormone receptor-positive tumors in Set A, RPPA detected an 866-fold difference in ERα between the tumor with the highest versus the lowest level of ERα. The maximal FC detected for PR was 142. This impressive dynamic range may result in RPPA identifying clinically relevant biomarkers that may not be predictive using IHC, or that may require a larger sample set to detect using IHC.

Protein-mRNA correlations

In cell lines and human tumors (Set B (**Supplemental Table 2**)), many phosphorylation and cleavage events were not well correlated with the corresponding transcript level (**Supplemental Table 3**). Thus, mRNA-based assays do not accurately characterize the functional proteome, underlining the necessity for a validated approach to study the functional proteome in cancer.

Discussion

Much progress has been made in genomic classification of breast cancer, with these results already impacting patient care.[1-10] However, proteins are the ultimate effectors of all cellular outcomes, and functional proteomic data represent an under-evaluated information resource for the identification of useful biomarkers in solid tumors. This is particularly relevant given that transcript levels do not correlate well with many post-translational protein modifications (e.g. phosphorylation, cleavage) in breast tumors and cell lines (**Supplemental Table 3**). RPPA represents an emerging functional proteomic assay that has the potential to provide a cost- and material-effective, high-throughput, comprehensive, sensitive and quantitative approach to molecular classification and pathophysiology studies.[11-18] RPPA has been demonstrated to have utility in the analysis of functional proteomic events in-vitro[11-18] and allows exploration of the intricacy of cellular signaling in a manner that cannot be accomplished by immunoblotting or IHC.

Although the application of RPPA to analysis of the functional proteome in cell lines and xenografts has proven relatively straightforward, the application of this technology to the study of human tumors presents a number of obstacles. These obstacles include intratumoral heterogeneity in protein expression and activation as well as variability in tissue handling after resection prior to freezing. Indeed, our study demonstrates that both intratumoral heterogeneity and increasing time to tissue freezing result in variability in detected protein levels in breast tumors. However, the reproducibility and robustness of RPPA, the faithfulness with which total and phosphoproteins and the functional proteomic 'fingerprint' are preserved in different sections derived from snap frozen primary breast tumors, and the surprising stability of this 'fingerprint' with increasing time to freezing all facilitate the application of RPPA to the accurate study of individual and multiple protein biomarkers in non-microdissected breast tumor specimens.

The primary purpose of this study was to address and overcome obstacles to the successful application of RPPA to the study of the breast cancer functional proteome. We selected 82 antibodies (**Supplemental Table 1**) that recognize multiple kinase and steroid signaling events and their downstream effectors because these proteins are important to breast carcinogenesis.[19-39] The validation of RPPA as a robust tool for the study of the functional proteome in cancer is important for a number of reasons. In addition to potential utility in the identification of prognostic and predictive biomarkers in breast cancer, RPPA has potential utility for the identification of baseline and pharmacodynamic biomarkers that predict benefit from novel therapies targeting kinase signaling pathways. Indeed, we have already established a preclinical

precedent for the latter approach[13] and are currently testing this model in an ongoing clinical trial of the Akt inhibitor perifosine in the treatment of women with advanced ovarian cancer.

Several questions remain to be answered. RPPA has advantages over IHC and immunoblotting, including throughput, cost, sensitivity, amount of material required, objective quantification and a superior dynamic range. However, since IHC provides information concerning spatial organization and RPPA does not, the integrated use of these approaches may provide a complementary approach to the study of functional proteomics in breast and other solid tumors. It is also unknown if independent analysis of microdissected solid tumor and stromal tissues will provide additional information concerning the functional proteome to that provided by the analysis of non-microdissected tissue as described herein. Since the routine storage of frozen tumor tissue is a relatively recent approach in most institutions, it should be determined if RPPA can be reliably applied to the study of the functional proteome in formalin fixed paraffin-embedded (FFPE) tumor tissue. Further, as the functional proteome is composed of many more proteins than are shown in **Supplemental Table 1**, additional high quality affinity reagents could greatly extend the utility of the technology. Ultimately, the true test of RPPA will lie in its ability to determine robust functional proteomic biomarkers that can impact clinical practice.

References

1. Sørlie, T., Perou, C.M., Tibshirani, R., Aas, T., Geisler, S., Johnsen, H., Hastie, T., Eisen, M.B., van de Rijn, M., Jeffrey, S.S., Thorsen, T., Quist, H., Matese, J.C., Brown, P.O., Botstein, D., Eystein Lønning, P., and Børresen-Dale, A.L. (2001) Gene expression patterns of breast carcinomas distinguish tumor subclasses with clinical implications. *Proc. Natl. Acad. Sci. U S A.* 98, 10869-10874
2. van de Vijver, M.J., He, Y.D., van't Veer, L.J., Dai, H., Hart, A.A., Voskuil, D.W., Schreiber, G.J., Peterse, J.L., Roberts, C., Marton, M.J., Parrish, M., Atsma, D., Witteveen, A., Glas, A., Delahaye, L., van der Velde, T., Bartelink, H., Rodenhuis, S., Rutgers, E.T., Friend, S.H., and Bernards, R. (2002) A Gene-Expression Signature as a Predictor of Survival in Breast Cancer. *N. Engl. J. Med.* 347, 1999-2009
3. Ayers, M., Symmans, W.F., Stec, J., Damokosh, A.I., Clark, E., Hess, K., Lecocke, M., Metivier, J., Booser, D., Ibrahim, N., Valero, V., Royce, M., Arun, B., Whitman, G., Ross, J., Sneige, N., Hortobagyi, G.N., and Pusztai, L. (2004) Gene expression profiles predict complete pathologic response to neoadjuvant paclitaxel and fluorouracil, doxorubicin, and cyclophosphamide chemotherapy in breast cancer. *J. Clin. Oncol*. 22, 2284-2293
4. Sjöblom, T., Jones, S., Wood, L.D., Parsons, D.W., Lin, J., Barber, T.D., Mandelker, D., Leary, R.J., Ptak, J., Silliman, N., Szabo, S., Buckhaults, P., Farrell, C., Meeh, P., Markowitz, S.D., Willis, J., Dawson, D., Willson, J.K., Gazdar, A.F., Hartigan, J., Wu, L., Liu, C., Parmigiani, G., Park, B.H., Bachman, K.E., Papadopoulos, N., Vogelstein, B.,

Kinzler, K.W., and Velculescu, V.E. (2006) The consensus coding sequences of human breast and colorectal cancers. *Science* 314, 268-274

5. Rosenwald, A., Wright, G., Chan, W.C., Connors, J.M., Campo, E., Fisher, R.I., Gascoyne, R.D., Muller-Hermelink, H.K., Smeland, E.B., Giltnane, J.M., Hurt, E.M., Zhao, H., Averett, L., Yang, L., Wilson, W.H., Jaffe, E.S., Simon, R., Klausner, R.D., Powell, J., Duffey, P.L., Longo, D.L., Greiner, T.C., Weisenburger, D.D., Sanger, W.G., Dave, B.J., Lynch, J.C., Vose, J., Armitage, J.O., Montserrat, E., López-Guillermo, A., Grogan, T.M., Miller, T.P., LeBlanc, M., Ott, G., Kvaloy, S., Delabie, J., Holte, H., Krajci, P., Stokke, T., and Staudt, L.M. Lymphoma/Leukemia Molecular Profiling Project. (2002) The Use of Molecular Profiling to Predict Survival after Chemotherapy for Diffuse Large-B-Cell Lymphoma. *N. Engl. J. Med*. 346, 1937-1947
6. Bullinger, L., Döhner, K., Bair, E., Fröhling, S., Schlenk, R.F., Tibshirani, R., Döhner, H., and Pollack, J.R. (2004) Use of Gene-Expression Profiling to Identify Prognostic Subclasses in Adult Acute Myeloid Leukemia. *N. Engl. J. Med*. 350, 1605-1616
7. Jazaeri, A.A., Yee, C.J., Sotiriou, C., Brantley, K.R., Boyd, J., and Liu, E.T. (2002) Gene expression profiles of BRCA1-linked, BRCA2-linked, and sporadic ovarian cancers. *J. Natl. Cancer Inst*. 94, 990-1000
8. Pedersen, N., Mortensen, S., Sørensen, S.B., Pedersen, M.W., Rieneck, K., Bovin, L.F., and Poulsen, H.S. (2003) Transcriptional gene expression profiling of small cell lung cancer cells. *Cancer Res*. 63, 1943-1953
9. Yu, Y.P., Landsittel, D., Jing, L., Nelson, J., Ren, B., Liu, L., McDonald, C., Thomas, R., Dhir, R., Finkelstein, S., Michalopoulos, G., Becich, M., and Luo, J.H. (2004) Gene

expression alterations in prostate cancer predicting tumor aggression and preceding development of malignancy. *J. Clin. Oncol*. 22, 2790-2799

10. Sirotnak, F.M., She, Y., Khokhar, N.Z., Hayes, P., Gerald, W., and Scher, H.I. (2004) Microarray analysis of prostate cancer progression to reduced androgen dependence: studies in unique models contrasts early and late molecular events. *Mol. Carcinog*. 41, 150-163
11. Tibes, R., Qiu, Y., Lu, Y., Hennessy, B., Andreeff, M., Mills, G.B., and Kornblau, S.M. (2006) Reverse phase protein array (RPPA): Validation of a novel proteomic technology and utility for analysis of primary leukemia specimens and hematopoietic stem cells. *Mol. Cancer Ther*. 5, 2512-2521
12. Sheehan, K.M., Calvert, V.S., Kay, E.W., Lu, Y., Fishman, D., Espina, V., Aquino, J., Speer, R., Araujo, R., Mills, G.B., Liotta, L.A., Petricoin, E.F. 3rd, and Wulfkuhle, J.D. (2005) Use of reverse phase protein microarrays and reference standard development for molecular network analysis of metastatic ovarian carcinoma. *Mol. Cell. Proteomics* 4, 346-355
13. Hennessy, B.T., Lu, Y., Poradosu, E., Yu, Q., Yu, S., Hall, H., Carey, M.S., Ravoori, M., Gonzalez-Angulo, A.M., Birch, R., Henderson, I.C., Kundra, V., and Mills, G.B. (2007) Pharmacodynamic markers of perifosine efficacy. *Clin. Cancer Res*. 13, 7421-7431
14. Cheng, K.W., Lu, Y. & Mills, G.B. Assay of Rab25 function in ovarian and breast cancers. *Methods Enzymol*. 403, 202-215 (2005).
15. Charboneau, L., Tory, H., Chen, T., Winters, M., Petricoin, E.F. 3rd, Liotta, L.A., and Paweletz, C.P. (2002) Utility of reverse phase protein arrays: applications to signalling pathways and human body arrays. *Brief. Funct. Genomic Proteomic*. 1, 305-315
16. Iwamaru, A., Kondo, Y., Iwado, E., Aoki, H., Fujiwara, K., Yokoyama, T., Mills, G.B., and Kondo, S. (2007) Silencing mammalian target of rapamycin signaling by small

interfering RNA enhances rapamycin-induced autophagy in malignant glioma cells. *Oncogene* 26, 1840-1851

17. Wulfkuhle, J.D., Edmiston, K.H., Liotta, L.A. & Petricoin, E.F 3rd. (2006) Technology insight: pharmacoproteomics for cancer—promises of patient-tailored medicine using protein microarrays. *Nat. Clin. Pract. Oncol*. 3, 256-268
18. Hu, J., He, X., Baggerly, K.A., Coombes, K.R., Hennessy, B.T., and Mills, G.B. (2007) Non-parametric quantification of protein lysate arrays. *Bioinformatics* 23, 1986-1994
19. Nagata, Y., Lan, K.H., Zhou, X., Tan, M., Esteva, F.J., Sahin, A.A., Klos, K.S., Li, P., Monia, B.P., Nguyen, N.T., Hortobagyi, G.N., Hung, M.C., and Yu, D. (2004) PTEN activation contributes to tumor inhibition by trastuzumab, and loss of PTEN predicts trastuzumab resistance in patients. *Cancer Cell* 6, 117-127
20. Saal, L.H., Holm, K., Maurer, M., Memeo, L., Su, T., Wang, X., Yu, J.S., Malmström, P.O., Mansukhani, M., Enoksson, J., Hibshoosh, H., Borg, A., and Parsons, R. (2005) PIK3CA mutations correlate with hormone receptors, node metastasis, and ERBB2, and are mutually exclusive with PTEN loss in human breast carcinoma. *Cancer Res*. 65, 2554-2559
21. Monni, O., Barlund, M., Mousses, S., Kononen, J., Sauter, G., Heiskanen, M., Paavola, P., Avela, K., Chen, Y., Bittner, M.L., and Kallioniemi, A. (2001) Comprehensive copy number and gene expression profiling of the 17q23 amplicon in human breast cancer. *Proc. Natl. Acad. Sci. U S A*. 98, 5711-5716
22. Bellacosa, A., de Feo, D., Godwin, A.K., Bell, D.W., Cheng, J.Q., Altomare, D.A., Wan, M., Dubeau, L., Scambia, G., Masciullo, V., Ferrandina, G., Benedetti Panici, P.,

Mancuso, S., Neri, G., and Testa, J.R. (1995) Molecular alterations of the AKT2 oncogene in ovarian and breast carcinomas. *Int. J. Cancer* 64, 280-285

23. Espina, V., Woodhouse, E.C., Wulfkuhle, J., Asmussen, H.D., Petricoin, E.F 3rd., and Liotta, L.A. (2004) Protein microarray detection strategies: focus on direct detection technologies. *J. Immunol. Methods* 290, 121-133
24. Neve, R.M., Chin, K., Fridlyand, J., Yeh, J., Baehner, F.L., Fevr, T., Clark, L., Bayani, N., Coppe, J.P., Tong, F., Speed, T., Spellman, P.T., DeVries, S., Lapuk, A., Wang, N.J., Kuo, W.L., Stilwell, J.L., Pinkel, D., Albertson, D.G., Waldman, F.M., McCormick, F., Dickson, R.B., Johnson, M.D., Lippman, M., Ethier, S., Gazdar, A., and Gray, J.W. (2006) A collection of breast cancer cell lines for the study of functionally distinct cancer subtypes. *Cancer Cell* 10, 515-527
25. Stoica, G.E., Franke, T.F., Moroni, M., Mueller, S., Morgan, E., Iann, M.C., Winder, A.D., Reiter, R., Wellstein, A., Martin, M.B., and Stoica, A. (2003) Effect of estradiol on estrogen receptor-alpha gene expression and activity can be modulated by the ErbB2/PI 3-K/Akt pathway. *Oncogene* 22, 7998-8011
26. Bachman, K.E., Argani, P., Samuels, Y., Silliman, N., Ptak, J., Szabo, S., Konishi, H., Karakas, B., Blair, B.G., Lin, C., Peters, B.A., Velculescu, V.E., and Park, B.H. (2004) The PIK3CA Gene is Mutated with High Frequency in Human Breast Cancers. *Cancer Biol. Ther*. 3, 772-775
27. Shou, J., Massarweh, S., Osborne, C.K., Wakeling, A.E., Ali, S., Weiss, H., and Schiff, R. (2004) Mechanisms of tamoxifen resistance: increased estrogen receptor-HER2/neu cross-talk in ER/HER2-positive breast cancer. *J. Natl. Cancer Inst*. 96, 926-935

28. Knuefermann, C., Lu, Y., Liu, B., Jin, W., Liang, K., Wu, L., Schmidt, M., Mills, G.B., Mendelsohn, J., and Fan, Z. (2003) HER2/PI-3K/Akt activation leads to a multidrug resistance in human breast adenocarcinoma cells. *Oncogene* 22, 3205-3212
29. Liang, K., Jin, W., Knuefermann, C., Schmidt, M., Mills, G.B., Ang, K.K., Milas, L., and Fan, Z. (2003) Targeting the phosphatidylinositol 3-kinase/Akt pathway for enhancing breast cancer cells to radiotherapy. *Mol. Cancer Ther*. 2, 353-360
30. Brown, R.E. (2002) HER-2/neu-Positive breast carcinoma: molecular concomitants by proteomic analysis and their therapeutic implications. *Ann. Clin. Lab. Sci*. 32, 12-21
31. Ueda, Y., Wang, S., Dumont, N., Yi, J.Y., Koh, Y., and Arteaga, C.L. (2004) Overexpression of HER2 (erbB2) in human breast epithelial cells unmasks transforming growth factor beta-induced cell motility. *J. Biol. Chem*. 279, 24505-24513
32. Bakin, A.V., Tomlinson, A.K., Bhowmick, N.A., Moses, H.L., and Arteaga, C.L. (2000) Phosphatidylinositol 3-kinase function is required for transforming growth factor beta-mediated epithelial to mesenchymal transition and cell migration. *J. Biol. Chem*. 275, 36803-36810
33. Zhao, J.J., Liu, Z., Wang, L., Shin, E., Loda, M.F., and Roberts, T.M. (2005) The oncogenic properties of mutant p110alpha and p110beta phosphatidylinositol 3-kinases in human mammary epithelial cells. *Proc. Natl. Acad. Sci. U S A*. 102, 18443-18448
34. Ellis, M.J., Coop, A., Singh, B., Mauriac, L., Llombert-Cussac, A., Jänicke, F., Miller, W.R., Evans, D.B., Dugan, M., Brady, C., Quebe-Fehling, E., and Borgs, M. (2001) Letrozole is more effective neoadjuvant endocrine therapy than tamoxifen for ErbB-1- and/or ErbB-2-positive, estrogen receptor-positive primary breast cancer: evidence from a phase III randomized trial. *J. Clin. Oncol*. 19, 3808-3816

35. Smith, I.E., Dowsett, M., Ebbs, S.R., Dixon, J.M., Skene, A., Blohmer, J.U., Ashley, S.E., Francis, S., Boeddinghaus, I., Walsh, G.; IMPACT Trialists Group. (2005) Neoadjuvant treatment of postmenopausal breast cancer with anastrozole, tamoxifen, or both in combination: the Immediate Preoperative Anastrozole, Tamoxifen, or Combined with Tamoxifen (IMPACT) multicenter double-blind randomized trial. *J. Clin. Oncol*. 23, 5108-5116

36. Allred, D.C., Harvey, J.M., Berardo, M., and Clark, G.M. (1998) Prognostic and predictive factors in breast cancer by immunohistochemical analysis. *Mod. Pathol*. 11, 155-168

37. Jirström, K., Stendahl, M., Rydén, L., Kronblad, A., Bendahl, P.O., Stål, O., and Landberg, G. (2005) Adverse effect of adjuvant tamoxifen in premenopausal breast cancer with cyclin D1 gene amplification. *Cancer Res*. 65, 8009-8016

38. Yamashita, H., Toyama, T., Nishio, M., Ando, Y., Hamaguchi, M., Zhang, Z., Kobayashi, S., Fujii, Y., and Iwase, H. (2006) p53 protein accumulation predicts resistance to endocrine therapy and decreased post-relapse survival in metastatic breast cancer. *Breast Cancer Res*. 8, R48

39. Paik, S., Shak, S., Tang, G., Kim, C., Baker, J., Cronin, M., Baehner, F.L., Walker, M.G., Watson, D., Park, T., Hiller, W., Fisher, E.R., Wickerham, D.L., Bryant, J., and Wolmark, N. (2004) A multigene assay to predict recurrence of tamoxifen-treated, node-negative breast cancer. *N. Engl. J. Med*. 351, 2817-2826

40. Danish Breast Cancer Cooperative Group, Nielsen, H.M., Overgaard, M., Grau, C., Jensen, A.R., and Overgaard, J. (2006) Study of failure pattern among high-risk breast cancer patients with or without postmastectomy radiotherapy in addition to adjuvant

systemic therapy: long-term results from the Danish Breast Cancer Cooperative Group DBCG 82 b and c randomized studies. *J. Clin. Oncol.* 24, 2268-2275

FIGURE LEGENDS

Figure 1. Antibody validation for reverse phase protein array (RPPA). MDAMB468, ZR75-1 and T47D cells were left untreated followed by no stimulation (control) or by stimulation with epidermal growth factor (EGF), or were treated with LY294002 (phosphatidylinositol-3-kinase (PI3K) inhibitor), perifosine (Akt inhibitor), rapamycin (mTOR inhibitor) or ultraviolet (UV) irradiation and then stimulated with epidermal growth factor (EGF) in the case of treatment with the three inhibitors. Lysates were then probed with antibody to total Akt (Figure 1A) or phospho(p)Akt at serine 473 (S473) (Figure 1B) by western blotting (membranes shown) and RPPA (nitrocellulose slides shown) and the derived signals for total and phosphorylated Akt were quantified. For RPPA, each lysate was arrayed in five serial twofold dilutions on nitrocellulose slides (with increasing dilution from left to right on each slide for each lysate). A control spot (a mixed cell line lysate) was placed at the end of each sample lysate's five serial twofold dilution series to give six spots. Four samples are arrayed in this fashion in each grid of 24 spots on the nitrocellulose slides shown. The correlation coefficients between signals derived using RPPA and western blotting for total and phosphorylated Akt were 0.897 and 0.93, respectively, as shown in the correlation plots. These correlation coefficients were based on 18 datapoints in each case and indicate valid antibodies for RPPA. Figures 1A and 1B also demonstrate the process of curve fitting that is applied by the R package SuperCurve (version 1.01)[18] for the purpose of deriving log2 protein concentrations for each protein lysate on the slide using the fit of each sample dilution series to the 'supercurve' (see Methods section for more details).

Figure 2. Reverse phase protein array (RPPA) reproducibility for four antibodies. Five serial twofold dilutions were made from 48 protein lysates (experimental outline shown in **Supplemental Figure 1**) and the serial dilutions were spotted in triplicate on three sets of nitrocellulose-coated slides at two timepoints ('technical replicates') separated by one month followed by probing of each slide set with four antibodies to determine intra-slide, inter-slide and inter-batch reproducibility, respectively. The individual correlation coefficients (R) for pairs of replicates for intra-slide, inter-slide and inter-batch reproducibility are shown under each correlation plot for each antibody.

Figure 3. Changes in proteins with increasing time to breast tumor freezing. Ten human breast tumors were collected immediately at surgery and frozen after increasing time intervals up until 24 hours. Of the 12 total and phosphoproteins shown, a progressive deterioration was seen with increasing time to breast tumor freezing in the phosphorylation of acetyl coenzyme A carboxylase (AcCoAp) and in the phosphorylation of AMP-activated protein kinase (AMPKp). In contrast, no significant change was seen with increasing time to tumor freezing in the expression of AcCoA, AMPK, cyclin B1 (CCNB1) or cyclin D1 (CCND1), or in the expression and phosphorylation of epidermal growth factor receptor (EGFR), Akt and glycogen synthase kinase 3 (GSK3). The expression of each total and phosphoprotein was expressed in log2 units on the Y axis of each plot and the time series is shown on the X axis of each plot (0, 0.5, 1, 2, 4, 6 and 24 hours (note that point 7 on the X axis corresponds to 24 hours between tumor resection and freezing)).

Figure 4. The reproducibility of clinically important breast cancer protein biomarkers detected by reverse phase protein array (RPPA) despite intratumoral heterogeneity. In two cohorts of separate sections derived from each of 49 non-microdissected hormone receptor-positive breast cancers, high expression of cyclin B1 and of p53 proteins as determined using RPPA (>log mean centered cutoff of 0) was associated with short disease-free survival times.

Figure 5. Stability of the primary human breast tumor functional proteomic 'fingerprint' despite variability resulting from intratumoral heterogeneity and tissue handling/time to tumor freezing. The overall total and phosphoprotein expression pattern or 'signature' was determined by unsupervised hierarchical clustering of data derived from reverse phase protein array (RPPA) analysis of ten primary human breast tumors using the antibodies shown in supplemental table 1. This 'signature' was faithfully preserved in the majority of cases across three separate immediately (snap) frozen (time 0) sections derived from each tumor (FT1-10) (A) and across nine separate sections frozen at increasing time delays after surgical resection up to 24 hours (B).

TABLES

Table 1. Time-dependent variability in total and phospho(p) protein expression with increasing time to breast tumor freezing. The expression of 21/82 total and phosphoproteins displayed significant time-dependent variability with increasing time to tumor freezing up to 24 hours. These 21 proteins are subdivided by function in this table.

Apoptosis: Cleaved caspase 7, cleaved PARP

Energy sensor pathway: AcCoAp (i.e. phospho-AcCoA), AMPKp, TSC2, TSC2p

Hormonal signaling: ERp167, PR

Phosphatidylinositol-3-kinase (PI3K) pathway: Aktp308, p110 alpha, PTEN

Src/mitogen activated protein kinase (MAPK) pathway: MAPKp, p38, p38p180_182, srcp527

Translation: p70S6 Kinase, S6p235-236

Other: B catenin, COX2, E cadherin, stat3p705

SUPPLEMENTAL FIGURE LEGENDS

Supplemental Figure 1. Experimental outline for the reverse phase protein array (RPPA) reproducibility experiment (Figure 2). Five serial twofold dilutions were made from 48 protein lysates and the serial dilutions were spotted in triplicate on three sets of nitrocellulose-coated slides at two timepoints separated by one month, followed by probing of each slide set with four antibodies to determine intra-slide, inter-slide and inter-batch reproducibility for the total and phosphoproteins detected by these four antibodies.

Supplemental Figure 2. Changes in total and phosphoproteins with increasing time to breast tumor freezing. Six western blots demonstrate stability of mitogen activated protein kinase (ERK2), Akt and AMP-activated protein kinase (AMPK) expression and of Akt phosphorylation (Aktp473) with increasing time to tumor freezing. In contrast, consistent with RPPA data (Supplemental Folder 1), a progressive deterioration was seen with increasing time to breast tumor freezing in the phosphorylation of mitogen activated protein kinase (MAPKp) and in the phosphorylation of AMPK (AMPKp). The time before tumor freezing is shown along the top of the figure.

Supplemental Figure 3. Stability of a human breast tumor functional proteomic 'fingerprint' despite individual protein variability resulting from intratumoral heterogeneity. This figure shows unsupervised clustering of total and phosphoprotein quantification data obtained by applying reverse phase protein arrays (RPPA) to protein lysates derived from two independent sections obtained from each of 49 human hormone

receptor-positive breast cancers. In only 6 of the 49 cases did the tumor functional proteomic 'fingerprints' in each of the two corresponding tumor sections not significantly correlate with each other.

SUPPLEMENTAL TABLES

Supplemental Table 1. Eighty-two monospecific antibodies used in this study.

Antibody name	Protein name	Company*	cat#	Host	Dilution
4EBP1	4E Binding Protein 1	Cell Signaling Technology, Inc.	CS 9452	Rabbit	1 in 100
4EBP1p37	4EBP1 phosphorylation at T37/T46	Cell Signaling Technology, Inc.	CS 9459	Rabbit	1 in 100
AcCoA	Acetyl CoA Carboxylase	Epitomics, Inc.	1768-1	Rabbit	1 in 250
AcCoAp	AcCoA phosphorylation at S79	Cell Signaling Technology, Inc.	CS 3661	Rabbit	1 in 250
Akt	Protein Kinase B	Cell Signaling Technology, Inc.	CS 9272	Rabbit	1 in 250
Aktp308	Akt phosphorylation at S308	Cell Signaling Technology, Inc.	CS 9275	Rabbit	1 in 250
Aktp473	Akt phosphorylation at S473	Cell Signaling Technology, Inc.	CS 9271	Rabbit	1 in 250
AMPK	AMPK	Cell Signaling Technology, Inc.	CS 2532	Rabbit	1 in 250
AMPKp	AMPK phosphorylation at S172	Cell Signaling Technology, Inc.	CS 2535	Rabbit	1 in 250
β catenin	B catenin	Cell Signaling Technology, Inc.	CS 9562	Rabbit	1 in 300
bcl2	bcl2	Dako	M0887	Mouse	1 in 200
BRCA1	BRCA1	Upstate Biotechnology, Inc.	07-434	Rabbit	1 in 1000
caveolin 1	Caveolin 1	Cell Signaling Technology, Inc.	CS 3232	Rabbit	1 in 250
CCNB1	Cyclin B1	Epitomics, Inc.	1495-1	Rabbit	1 in 500
CCND1	Cyclin D1	Santa Cruz Biotechnology, Inc.	SC-718	Rabbit	1 in 1000
CCNE1	Cyclin E1	Santa Cruz Biotechnology, Inc.	SC-247	Mouse	1 in 500
CD31	CD31	Dako	M0823	Mouse	1 in 500
CDK4	CDK4	Cell Signaling Technology, Inc.	CS 2906	Rabbit	1 in 250
cjun	Cjun	Cell Signaling Technology, Inc.	CS 9165	Rabbit	1 in 250
ckit	Ckit	Cell Signaling Technology, Inc.		Rabbit	1 in 150
cleaved caspase 7	Cleaved caspase 7 (Asp198)	Cell Signaling Technology, Inc.	CS 9491	Rabbit	1 in 150
cleaved PARP	Cleaved PARP (Asp214)	Cell Signaling Technology, Inc.	CS 9546	Mouse	1 in 250
cmyc	Cmyc	Cell Signaling Technology, Inc.	CS 9402	Rabbit	1 in 150
Collagen VI	Collagen VI	Santa Cruz Biotechnology, Inc.	SC-20649	Rabbit	1 in 750
COX2	COX2	Epitomics, Inc.	2169-1	Rabbit	1 in 500

E cadherin	E cadherin	Cell Signaling Technology, Inc.	CS 4065	Rabbit	1 in 200
EGFR	Epidermal growth factor receptor	Santa Cruz Biotechnology, Inc.	SC-03	Rabbit	1 in 200
EGFRp1045	EGFR phosphorylation at Y1045	Cell Signaling Technology, Inc.	CS 2237	Rabbit	1 in 100
EGFRp922	EGFR phosphorylation at Y992	Cell Signaling Technology, Inc.	CS 2235	Rabbit	1 in 100
ER	Estrogen receptor alpha	Lab Vision Coorporation (formerly Neomarkers)	Sp1	Rabbit	1 in 250
ERK2	Mitogen-activated protein kinase	Cell Signaling Technology, Inc.	SC-154	Rabbit	1 in 250
ERp118	ER phosphorylation at S118	Epitomics, Inc.	1091-1	Rabbit	1 in 200
ERp167	ER phosphorylation at S167	Epitomics, Inc.	2492-1	Rabbit	1 in 200
GSK3	Glycogen synthase kinase 3 beta	Santa Cruz Biotechnology, Inc.	SC-7291	Mouse	1 in 1000
GSK3p21_9	GSK3 phosphorylation at S21/S9	Cell Signaling Technology, Inc.	CS 9331	Rabbit	1 in 250
HER2	Human epidermal receptor 2	Epitomics, Inc.	1148-1	Rabbit	1 in 250
HER2p1248	HER2 phosphorylation at Y1248	Upstate Biotechnology, Inc.	06-229	Rabbit	1 in 750
IGF1R	Insulin-like growth factor receptor 1	Cell Signaling Technology, Inc.	CS 3027	Rabbit	1 in 500
IGFRp	IGF1R phosphorylation at Y1135/Y1136	Cell Signaling Technology, Inc.	CS 3024	Rabbit	1 in 200
JNK	cjun N terminal Kinase	Santa Cruz Biotechnology, Inc.	SC-474	Rabbit	1 in 200
JNKp183-185	JNK phosphorylation at T183/Y185	Cell Signaling Technology, Inc.	CS 9251	Rabbit	1 in 150
MAPKp	MAPK1/2 phosphorylation at T202/T204	Cell Signaling Technology, Inc.	CS 4377	Rabbit	1 in 1000
MEK1	MAPK/ERK kinase 1	Epitomics, Inc.	1235-1	Rabbit	1 in 15000
MEK12p	MEK1/2 phosphorylation at T217/T221	Cell Signaling Technology, Inc.	CS 9121	Rabbit	1 in 800
mTOR	mammalian target of rapamycin	Cell Signaling Technology, Inc.	CS 2983	Rabbit	1 in 400
p110alpha	p110alpha subunit of phosphatidylinositol-3-kinase	Epitomics, Inc.	1683-1	Rabbit	1 in 500
p21	p21	Santa Cruz Biotechnology, Inc.	SC-397	Rabbit	1 in 250
p27	p27	Santa Cruz Biotechnology, Inc.	SC-527	Rabbit	1 in 500
p38	p38 MAPK	Cell Signaling Technology, Inc.	CS 9212	Rabbit	1 in 300
p38p180_2	p38 MAPK phosphorylation at T180/T182	Cell Signaling Technology, Inc.	CS 9211	Rabbit	1 in 250
p53	p53	Cell Signaling Technology, Inc.	CS 9282	Rabbit	1 in 3000
p7056 Kinase	p70S6 Kinase	Epitomics, Inc.	1494-1	Rabbit	1 in 500
p70S6Kp389	p70S6 Kinase phosphorylation at T389	Cell Signaling Technology, Inc.	CS 9205	Rabbit	1 in 200
PAI1	Plasminogen activator inhibitor-1	BD Biosciences	612024	Mouse	1 in 1000

pcmyc	cmyc phosphorylation at T58/S62	Cell Signaling Technology, Inc.	CS 9401	Rabbit	1 in 150
PDK1	Phosphoinositide Dependent Kinase 1	Cell Signaling Technology, Inc.	CS 3062	Rabbit	1 in 250
PDK1p241	PDK1 phosphorylation at S241	Cell Signaling Technology, Inc.	CS 3061	Rabbit	1 in 500
PKCalpha	Protein Kinase C alpha	Upstate Biotechnology, Inc.	05-154	Mouse	1 in 2000
PKCaphap657	PKCalpha phosphorylation at S657	Upstate Biotechnology, Inc.	06-822	Rabbit	1 in 3000
pmTOR	mTOR phosphorylation at S2448	Cell Signaling Technology, Inc.	CS 2971	Rabbit	1 in 150
PR	Progesterone receptor	Epitomics, Inc.	1483-1	Rabbit	1 in 400
PTEN	PTEN	Cell Signaling Technology, Inc.	CS 9552	Rabbit	1 in 500
Rab25	Rab25	Courtesy Dr. Kwai Wa Cheng, MDACC	Covance	Rabbit	1 in 4000
Rb	Retinoblastoma	Cell Signaling Technology, Inc.	CS 9309	Mouse	1 in 3000
Rbp	Rb phosphorylation at S807/S811	Cell Signaling Technology, Inc.	CS 9308	Rabbit	1 in 250
S6	S6 ribosomal protein	Cell Signaling Technology, Inc.	CS 2217	Rabbit	1 in 200
S6p235-236	S6 phosphorylation at S235/S236	Cell Signaling Technology, Inc.	CS 2211	Rabbit	1 in 3000
S6p240_4	S6 phosphorylation at S240/S244	Cell Signaling Technology, Inc.	CS 2215	Rabbit	1 in 3000
SGK	Serum Glucocorticoid Kinase	Cell Signaling Technology, Inc.	CS 3272	Rabbit	1 in 250
SGKp	SGK phosphorylation at S78	Cell Signaling Technology, Inc.	CS 3271	Rabbit	1 in 250
src	Src	Upstate Biotechnology, Inc.	05-184	Mouse	1 in 200
srcp416	src phosphorylation at Y416	Cell Signaling Technology, Inc.	CS 2101	Rabbit	1 in 150
srcp527	src phosphorylation at Y527	Cell Signaling Technology, Inc.	CS 2105	Rabbit	1 in 400
stat3	Signal transducer and activator of transcription 3	Upstate Biotechnology, Inc.	06-596	Rabbit	1 in 500
stat3p705	stat3 phosphorylation at S705	Cell Signaling Technology, Inc.	CS 9131	Rabbit	1 in 500
stat3p727	stat3 phosphorylation at S727	Cell Signaling Technology, Inc.	CS 9134	Rabbit	1 in 250
stat6p641	stat6 phosphorylation at Y641	Cell Signaling Technology, Inc.	CS 9361	Rabbit	1 in 150
stathmin	Stathmin	Epitomics, Inc.	1972-1	Rabbit	1 in 500
TSC2	Tuberous Sclerosis Kinase 2	Epitomics, Inc.	1613-1	Rabbit	1 in 500
TSC2p	TSC2 phosphorylation at T1462	Cell Signaling Technology, Inc.	CS 3617	Rabbit	1 in 200
VEGFR2	KDR2 / VEGF Receptor 2	Cell Signaling Technology, Inc.	CS 2479	Rabbit	1 in 700
XIAP	X linked inhibitor of apoptosis	Cell Signaling Technology, Inc.	CS 2042	Rabbit	1 in 200

*
Companies

Abcam, Inc. (Cambridge, MA)
BD Biosciences (San Jose, CA)
Cell Signaling Technology, Inc. (Danvers, MA)
Dako (Carpinteria, CA)
Epitomics, Inc. (Burlingame, CA)
Santa Cruz Biotechnology, Inc. (Santa Cruz, CA)
Upstate Biotechnology, Inc. (Millipore)

Supplemental Table 2. Clinical details of human breast tumors utilized in this study. CMF- cyclophosphamide, methotrexate, fluorouracil; Lum-luminal; MDACC-M. D. Anderson Cancer Center. In the Danish DBCG82 b and c breast cancer studies (Set B), premenopausal women with high-risk breast cancer were randomized to receive radiation therapy plus CMF (cyclophosphamide, methotrexate, fluorouracil) or to CMF chemotherapy alone, and postmenopausal women with high-risk breast cancer were randomized to receive radiation therapy plus tamoxifen (30 mg daily for 1 year) or tamoxifen alone (PMID: 10335782).

Breast tumor sample set: Origin	Set A: MDACC	Set B: DBCG82 b/c
Patient number	95	128
Tumor subtype		
Hormone receptor (HR)-positive	64	42 (LumA) 27 (LumB) 17 (Normal-like)
HER2-positive	10	18 (erbB2)
Triple (receptor)-negative	21	24 (basal)
Stage		
Unknown	0	0
Ductal carcinoma in situ (DCIS)	3	0
1	17	1
2	46	63
3	22	64
4	7	0
Grade		
1	6	19
2	38	52
3	49	30
Unknown	2	27
Adjuvant treatment		
Tamoxifen	19	77
Aromatase inhibitor	38	0
Cytotoxic chemotherapy	65 (anthracycline	51 (CMF)

Trastuzumab	and/or taxane) 1	0

Supplemental Table 3. Eighty two protein-mRNA correlation coefficients (rho) and corresponding p values. Proteins were quantified with reverse phase protein arrays (RPPA). Clearly, mRNA levels (from AB arrays) frequently do not correlate well with protein function (e.g. phosphorylation, cleavage) in cell lines or human tumors. It is also notable that protein-mRNA correlations are not consistent between human breast tumors and breast cancer cell lines for certain proteins. This may be related in part to the presence of stroma in human tumors but not in cell lines (e.g. with collagen VI and caveolin 1). In addition, the rho value for the PTEN protein-mRNA correlation is clearly poorer in human tumors than in cell lines, possibly related in part to the presence of significant amounts of PTEN in endothelial cells in human tumors.

Protein	Rho (128 human breast tumors)	P value (128 human breast tumors)	rho (52 breast cancer cell lines)	P value (52 breast cancer cell lines)
4EBP1	0.51	5.9E-12	0.688	0.000000875
4EBP1p37	0.43	0.000000025	0.736	0.000000141
AcCoA	0.37	0.0000022	0.6	0.0000302
AcCoAp	0.32	0.000042	0.594	0.0000385
Akt	0.33	0.000028	0.592	0.0000415
Aktp308	0.15	0.0503	-0.262	0.09
Aktp473	0.14	0.07	-0.186	0.231
AMPK	0.29	0.0002	0.0314	0.841
AMPKp	0.17	0.03	-0.153	0.328
B.catenin	0.2	0.03	0.134	0.389
bcl2	-0.03	0.72	0.211	0.174
BRCA1	0.24	0.002	0.322	0.0355
caveolin.1	0.47	3.2E-10	0.845	0
CCNB1	0.68	0	0.573	0.0000791
CCND1	0.52	1.5E-12	0.84	1.87E-12
CCNE1	0.59	2.2E-16		N/A
CD31	N/A	N/A	0.151	0.332
CDK4	0.13	0.09	0.39	0.0102

Cjun	0.14	0.08	0.491	0.000955
Ckit	0.68	0	0.36	0.0182
cleaved.caspase.7	0.14	0.08	0.159	0.308
cleaved.PARP	0.08	0.15	-0.262	0.0896
Cmyc	0.41	0.000000078	0.52	0.000419
Collagen.VI	0.09	0.28	0.394	0.00933
COX2	0.34	0.000013	N/A	N/A
E.cadherin	0.11	0.18	0.811	0
EGFR	0.42	0.000000038	0.576	0.0000725
EGFRp1068	0.01	0.85	0.0107	0.945
EGFRp922	-0.01	0.9	0.212	0.173
ER	0.85	0	0.621	0.0000137
ERK2	-0.04	0.66	0.381	0.0121
ERp118	0.35	0.0000084	N/A	N/A
ERp167	0.09	0.24	N/A	N/A
GSK3	0.08	0.34	0.37	0.0151
GSK3p21.9	-0.08	0.32	0.0474	0.762
HER2	0.75	0	0.707	0.000000413
HER2p1248	0.72	0	N/A	N/A
IGF1R	0.65	0	0.522	0.000403
IGFRp	0.04	0.65	N/A	N/A
JNK	0.04	0.59	0.0282	0.857
JNKp	-0.08	0.31	-0.0914	0.559
MAPKp	-0.1	0.22	-0.461	0.00187
MEK1	0.2	0.01	0.646	0.00000509
MEK12p	-0.08	0.33	0.301	0.0501
mTOR	0.04	0.64	0.486	0.0011
p110alpha	0.13	0.11	0.326	0.0336
p21	0.07	0.36	0.156	0.318
p27	0.1	0.22	0.0689	0.66
p38	0.001	0.99	0.194	0.213
p38p180.2	-0.03	0.71	-0.0741	0.636
p53	0.15	0.06	0.716	0.00000029
p7056.Kinase	0.54	1.4E-13	0.672	0.00000171
p70S6Kp389	-0.1	0.23	0.291	0.0584
PAI1	0.06	0.46	0.643	0.00000579

pcmyc		0.23		0.004		0.418	0.00566
PDK1		-0.13		0.11		0.0136	0.931
PDK1p241		-0.08		0.34		-0.0637	0.684
PKCalpha		0.08		0.31		0.812	0
PKCaphap657		0.03		0.73		0.808	0
pmTOR		0.04		0.61		0.357	0.0189
PR		0.74		0		0.634	0.00000841
PTEN		0.22		0.005		0.642	0.00000601
Rab25		0.25		0.001		0.755	6.63E-08
Rb		0.15		0.06		0.56	0.000123
Rbp		0.05		0.5		0.648	0.00000469
S6		-0.08		0.34		0.286	0.0632
S6p235.236		-0.13		0.11		0.0521	0.739
S6p240.4		-0.12		0.13		0.00211	0.989
SGK		0.56		3.8E-14	N/A		N/A
SGKp		0.16		0.05	N/A		N/A
src		-0.04		0.6		0.548	0.000178
srcp416		0.13		0.11		0.361	0.0178
srcp527		0.17		0.03		0.326	0.0333
stat3		0.22		0.004		0.416	0.00581
stat3p705		0.03		0.73		0.299	0.0515
stat3p727		-0.02		0.76		0.677	0.00000061
stat6p641		0.09		0.26		0.0177	0.91
stathmin		0.13		0.1	N/A		N/A
TSC2		0.11		0.17		0.317	0.0389
TSC2p		0.003		0.97		0.114	0.467
VEGFR2		0.15		0.06		0.0375	0.811
XIAP	N/A		N/A		N/A		N/A

Supplemental Table 4. Inter- versus intratumoral heterogeneity. The effects of intratumoral and intertumoral variability on breast cancer protein and phosphoprotein expression were tested by applying analysis of variance (ANOVA) models to reverse phase protein array (RPPA) data derived from 10 breast tumors that were each divided into three separate pieces with assistance from a breast pathologist that were frozen immediately after surgical excision. Column A=ANOVA p-value for inter-tumor variability; Column B= ANOVA p-value for intra-tumor variability; Column C= Maximum Intertumoral Fold Change; Column D= Mean Intratumoral Fold Change. Fold change is presented on a log2 scale. Of 82 proteins in three time 0 breast tumor replicates, the expression of 80 total and phosphoproteins demonstrated significant (ANOVA $p \leq 0.05$) variability across the ten different breast cancers (all except EGFRp1045 and JNK), while the expression of only 8 total and phosphoproteins demonstrated significant intratumoral variability within these primary breast tumors (B catenin, Collagen VI, EGFR, MAPKp, PTEN, Rbp, srcp527, stat3p705).

Protein	A	B	C	D
4EBP1	0	0.1219	2.47	0.52
4EBP1p37	0	0.94719	2.55	0.47
AcCoA	0	0.17774	4.15	0.79
AcCoAp	0	0.11817	4.4	0.85
Akt	0.00029	0.95098	1.51	0.41
Aktp308	0.00002	0.25644	3.57	0.72
Aktp473	0.00261	0.35564	3.21	0.91
AMPK	0.01602	0.83813	2.28	0.53
AMPKp	0.00009	0.84344	2.15	0.56
B.catenin	0	0.00737	3.18	0.49
Bcl2	0	0.24915	4.46	0.87
BRCA1	0.01167	0.74802	2.35	0.71
caveolin.1	0.00001	0.06764	4.99	1.19
CCNB1	0	0.54217	4.72	0.72
CCND1	0	0.88443	2.31	0.27

CCNE1	0	0.07275	3.98	0.5
CD31	0	0.18066	4.39	0.6
CDK4	0	0.11566	1.75	0.34
cjun	0.00001	0.84812	3	0.57
ckit	0	0.765	6.32	1.06
cleaved.caspase.7	0	0.42661	3.73	0.45
cleaved.PARP	0.00004	0.72989	3.64	0.84
cmyc	0.00006	0.45661	1.95	0.45
Collagen.VI	0	0.01389	6.17	1.2
COX2	0.00041	0.1167	1.76	0.49
E.cadherin	0	0.45206	2.79	0.53
EGFR	0	0.02095	2.87	0.47
EGFRp1045	0.08967	0.57635	6.49	1.75
EGFRp922	0.00011	0.72074	3.94	0.8
ER	0	0.30028	6.78	1.17
ERK2	0.00003	0.69498	2.6	0.54
ERp118	0.00001	0.37716	4.04	0.9
ERp167	0.00001	0.09904	1.74	0.3
GSK3	0.00002	0.69576	3.17	0.57
GSK3p21.9	0.00002	0.25323	6.84	1.38
HER2	0	0.10058	10.25	1.2
HER2p1248	0	0.16499	7.04	0.77
IGF1R	0	0.73024	3.5	0.45
IGFRp	0.00446	0.28133	2.72	0.65
JNK	0.05615	0.99488	2.06	0.58
JNKp	0	0.11185	2.88	0.32
MAPKp	0	0.03292	4.38	0.96
MEK1	0.00003	0.66118	1.65	0.42
MEK12p	0.00026	0.97569	1.21	0.35
mTOR	0	0.45838	2.44	0.33
p110alpha	0	0.96268	1.97	0.31
p21	0.00007	0.71856	2.47	0.4
p27	0	0.27306	2.18	0.28
p38	0.00049	0.47474	1.68	0.39
p38p180.2	0.00002	0.49019	2.74	0.63
p53	0.00456	0.96661	5.07	0.95

p7056.Kinase	0.00023	0.24569	2.25	0.4
p70S6Kp389	0.01012	0.30403	1.66	0.45
PAI1	0.00002	0.75364	5.63	0.66
pcmyc	0.0041	0.63759	1.96	0.46
PDK1	0	0.30491	1.5	0.31
PDK1p241	0.00002	0.28734	1.64	0.39
PKCalpha	0	0.40225	2.58	0.55
PKCaphap657	0.00001	0.15371	2.48	0.53
pmTOR	0.00018	0.50565	2.87	0.5
PR	0.00001	0.53572	6.05	0.88
PTEN	0.0002	0.04241	2.49	0.5
Rab25	0	0.89192	2.7	0.45
Rb	0.00852	0.63485	2.03	0.63
Rbp	0.00082	0.0172	6.86	2.19
S6	0	0.45463	3.9	0.72
S6p235.236	0	0.62345	2.8	0.61
S6p240.4	0	0.64948	3.92	0.71
SGK	0.00266	0.19466	2.77	0.86
SGKp	0.00004	0.80613	4.87	0.89
Src	0	0.90358	3.04	0.5
Srcp416	0.00386	0.96558	4.91	1.01
Srcp527	0	0.01943	1.7	0.39
Stat3	0	0.65719	2.61	0.34
Stat3p705	0	0.0244	2.68	0.42
Stat3p727	0	0.75202	6.09	0.52
Stat6p641	0.04498	0.44092	3.47	0.91
Stathmin	0.02785	0.94217	2.11	0.55
TSC2	0	0.1177	1.81	0.28
TSC2p	0.00004	0.42417	1.4	0.25
VEGFR2	0	0.05401	1.48	0.26
XIAP	0.00012	0.92235	2.68	0.56

Supplemental Table 5. Reproducibility associated with biologic replicates in reverse phase protein arrays (RPPA).

Correlation coefficients for the expression of fifty-two proteins and phosphoproteins across two independent sections obtained from each of 49 frozen human hormone receptor-positive breast cancers are shown in column A.

Antibody	A
AcCoAp	0.642918568
Akt	0.618759766
Aktp308	0.254004137
Aktp473	0.410063812
AMPK	0.513727089
AMPKp	0.536678994
B catenin	0.730700092
BADp	0.369340325
CCNB1	0.870882305
CCND1	0.625891268
Cleaved caspase 7	0.633270435
E cadherin	0.6183121
EGFR	0.68801607
EGFRp1068	0.405450715
ER	0.841639703
ERK2	0.736704897
ERp118	0.430508819
FKHRL1p318	0.691993326
GSK3	0.678269861
GSK3p21_9	0.592290954
HER2	0.217455474
HER2p1248	0.403034203
IGFR1	0.595481674
IGFR1p	0.436972091
JNK	0.424603378
JNKp183_5	0.543731864
MAPKp	0.79987626
MEK	0.579451091
MEK1-2p	0.659646302

mTOR	0.626602561
p110alpha	0.436998926
p27	0.849943011
p38	0.716704432
p38p180_2	0.608686332
p53	0.655654172
p70S6 Kinase	0.649534728
p70S6Kp389	0.115625786
PKCalphap657	0.58393973
pmTOR	0.006433235
PR	0.758475654
PTEN	0.529437664
Rab25	0.769013148
S6p235-236	0.720622398
S6p240_4	0.866983533
Src	0.71789969
srcp416	0.210019805
srcp527	0.625513318
stat3p705	0.539502613
stat3p727	0.550006586
stat6p	0.287410482
TSC2	0.647454784
TSC2p	0.538756346

Cutoff for significance
0.282 (p=0.05)
0.46 (p=0.001)

FIGURE 1

1A

Status:Valid

AKT

Cell Signaling #9272 Lot 1--21.13

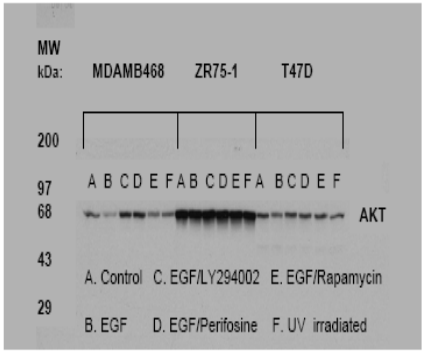

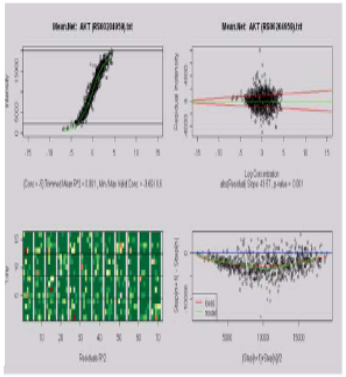

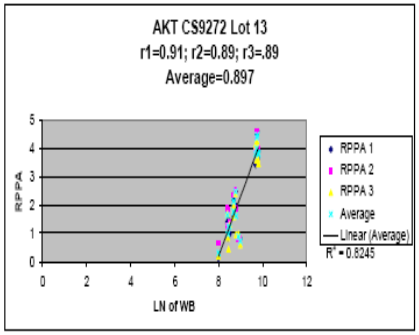

Dilutions: WB: 1:1000 RPPA: 1:250

July 20, 2007

1B

Status: Valid

AKTp473

Cell Signaling # 9271 Lot 10--23.10

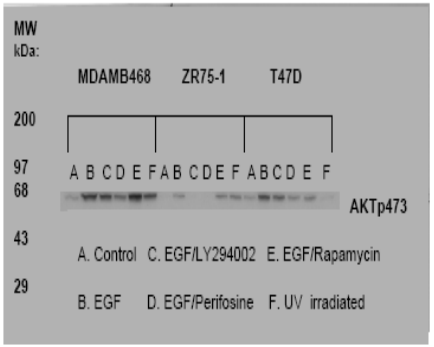

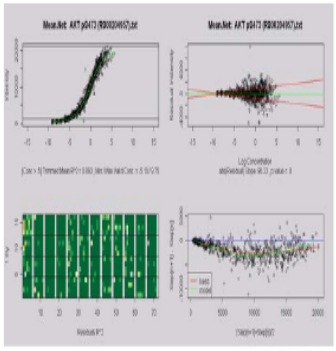

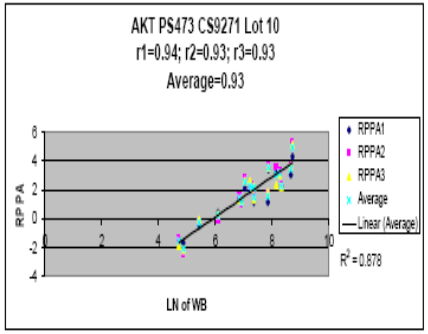

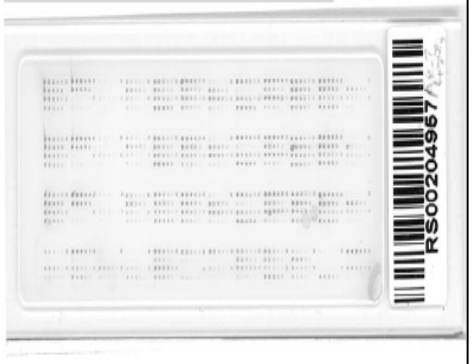

Dilutions: WB: 1:1000 RPPA: 1:250

July 20, 2007

FIGURE 2

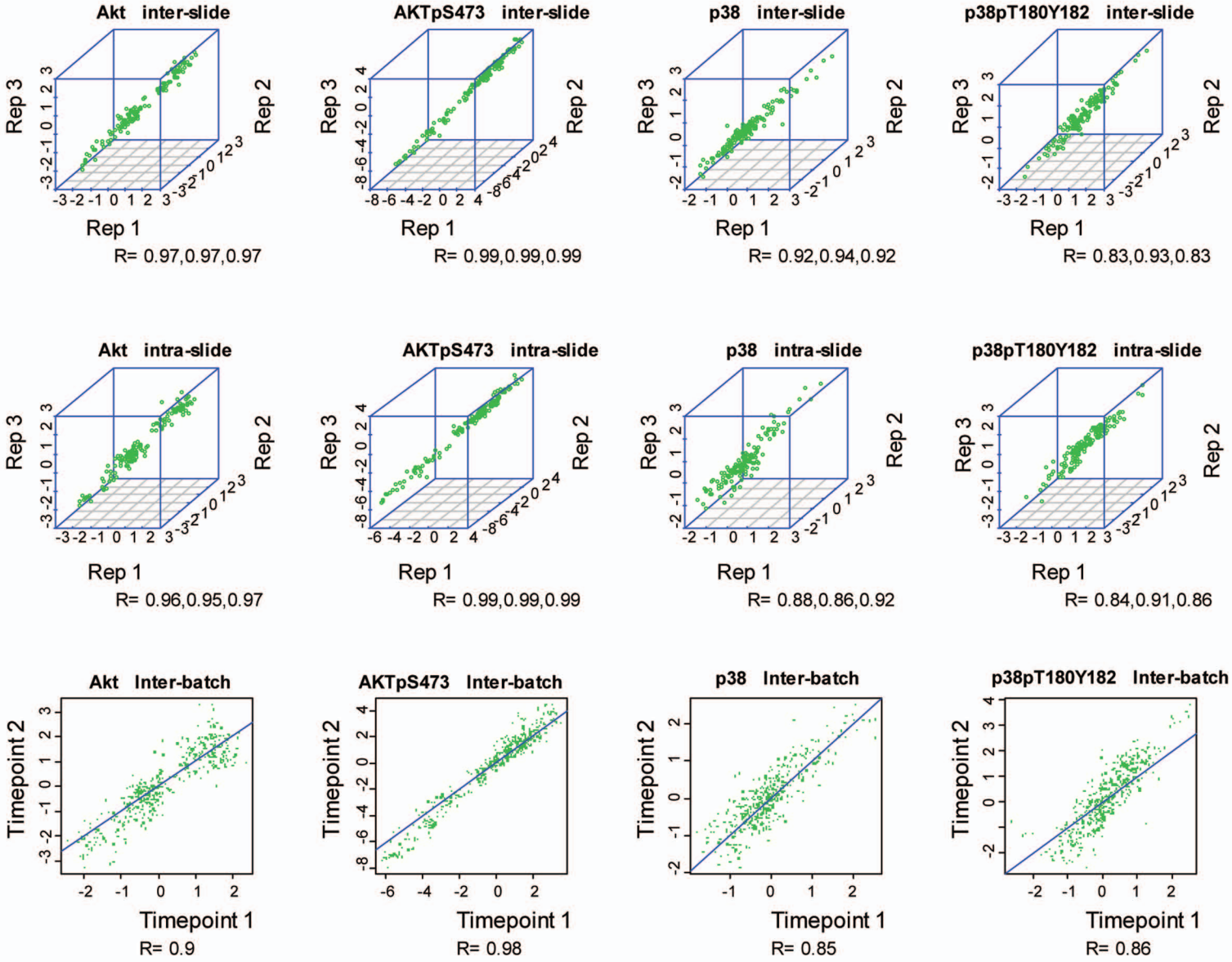
Akt inter-slide
Rep 3
Rep 2
Rep 1
R= 0.97,0.97,0.97
AKTpS473 inter-slide
Rep 3
Rep 2
Rep 1
R= 0.99,0.99,0.99
p38 inter-slide
Rep 3
Rep 2
Rep 1
R= 0.92,0.94,0.92
p38pT180Y182 inter-slide
Rep 3
Rep 2
Rep 1
R= 0.83,0.93,0.83
Akt intra-slide
Rep 3
Rep 2
Rep 1
R= 0.96,0.95,0.97
AKTpS473 intra-slide
Rep 3
Rep 2
Rep 1
R= 0.99,0.99,0.99
p38 intra-slide
Rep 3
Rep 2
Rep 1
R= 0.88,0.86,0.92
p38pT180Y182 intra-slide
Rep 3
Rep 2
Rep 1
R= 0.84,0.91,0.86
Akt Inter-batch
Timepoint 2
Timepoint 1
R= 0.9
AKTpS473 Inter-batch
Timepoint 2
Timepoint 1
R= 0.98
p38 Inter-batch
Timepoint 2
Timepoint 1
R= 0.85
p38pT180Y182 Inter-batch
Timepoint 2
Timepoint 1
R= 0.86

FIGURE 3

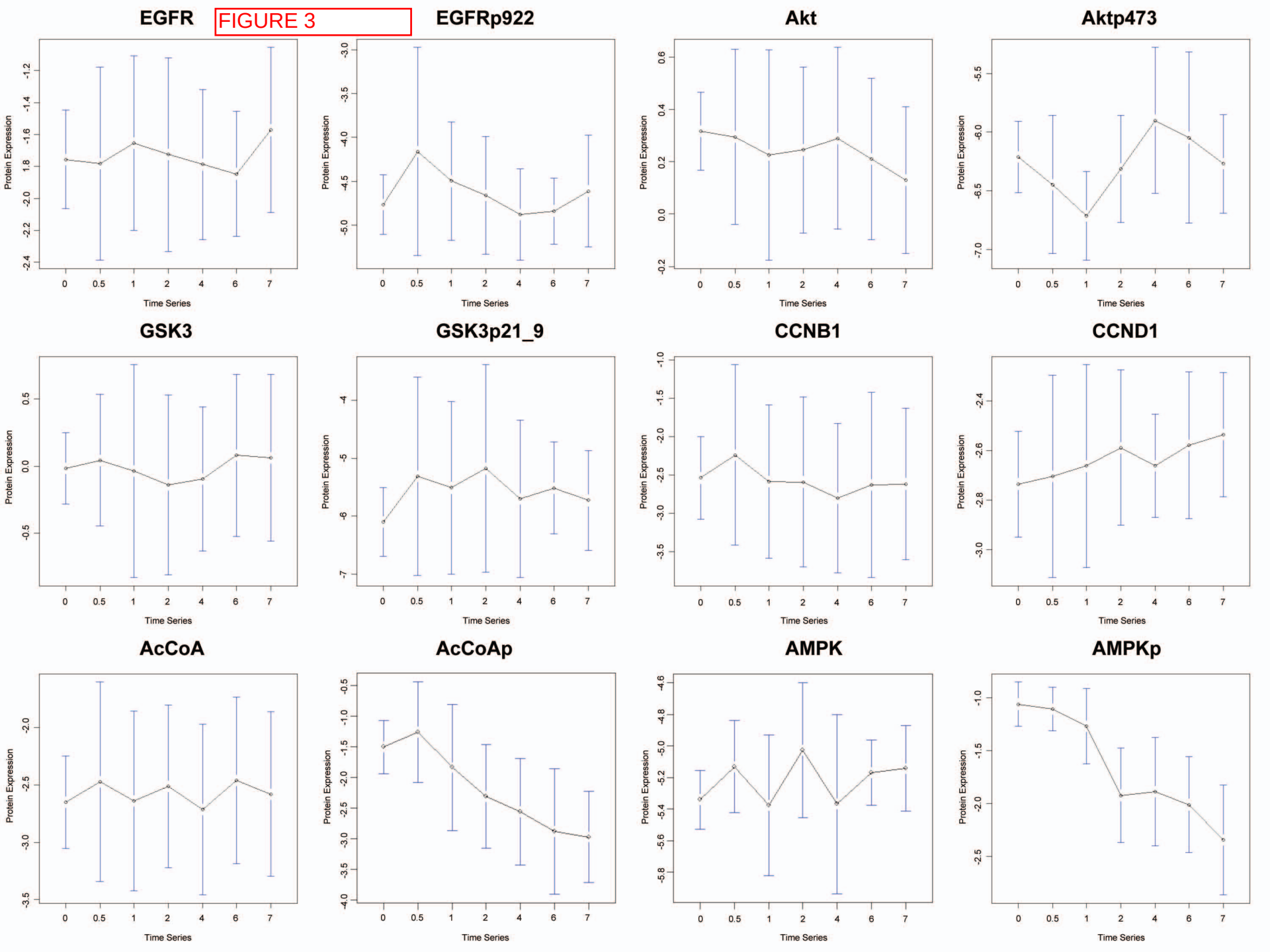
EGFR
EGFRp922
Akt
Aktp473
GSK3
GSK3p21_9
CCNB1
CCND1
AcCoA
AcCoAp
AMPK
AMPKp
Protein Expression
Time Series
0
0.5
1
2
4
6
7

FIGURE 4

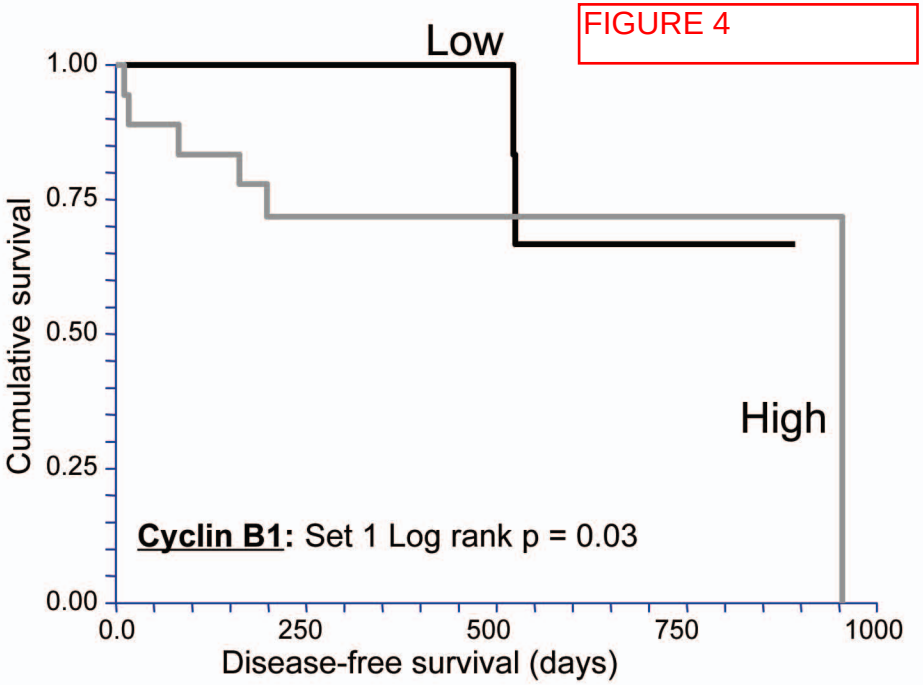
Low
High
1.00
0.75
0.50
0.25
0.00
Cumulative survival
0.0
250
500
750
1000
Disease-free survival (days)
Cyclin B1: Set 1 Log rank p = 0.03

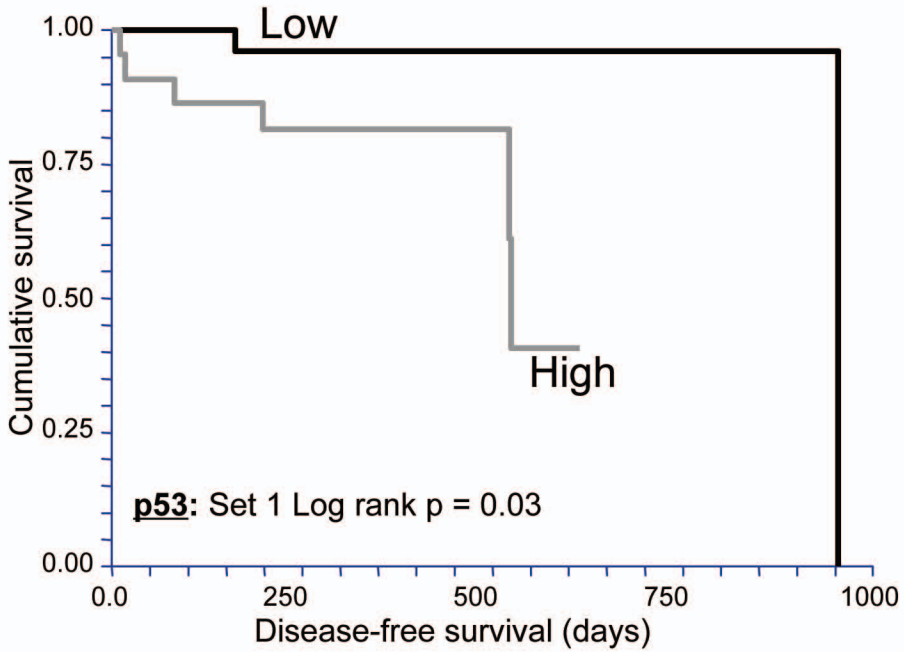
Low
High
1.00
0.75
0.50
0.25
0.00
Cumulative survival
0.0
250
500
750
1000
Disease-free survival (days)
p53: Set 1 Log rank p = 0.03

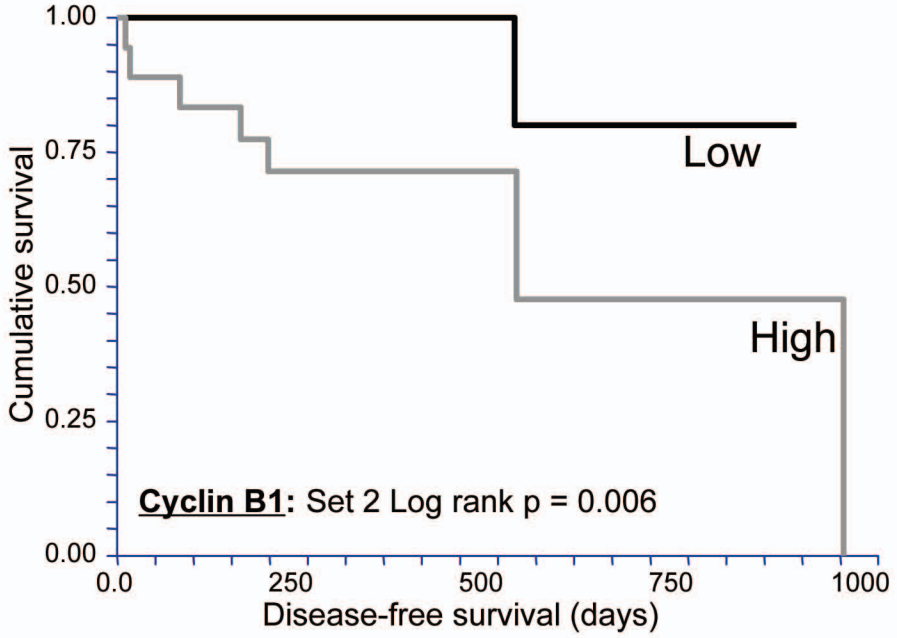
Low
High
1.00
0.75
0.50
0.25
0.00
Cumulative survival
0.0
250
500
750
1000
Disease-free survival (days)
Cyclin B1: Set 2 Log rank p = 0.006

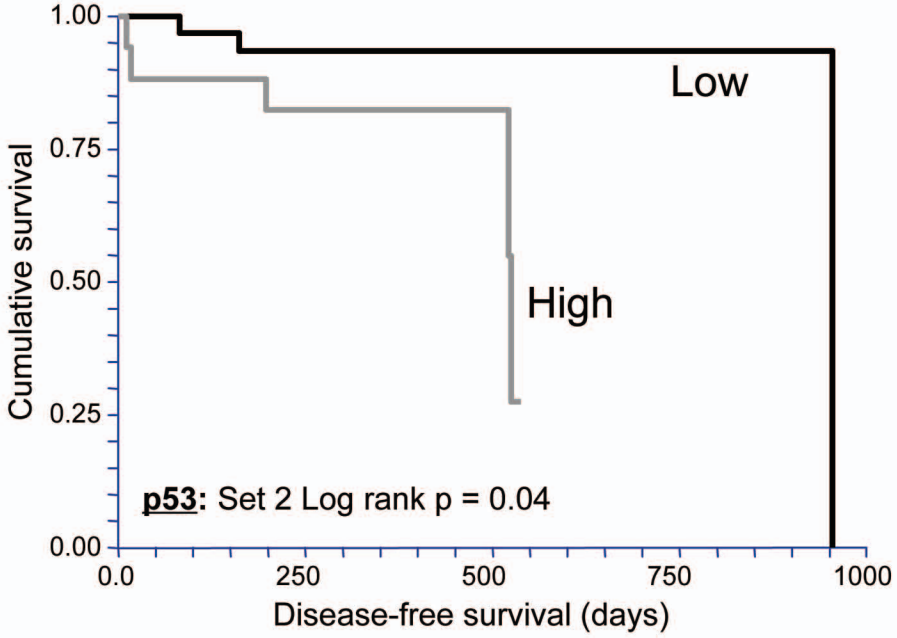
Low
High
1.00
0.75
0.50
0.25
0.00
Cumulative survival
0.0
250
500
750
1000
Disease-free survival (days)
p53: Set 2 Log rank p = 0.04

FIGURE 5

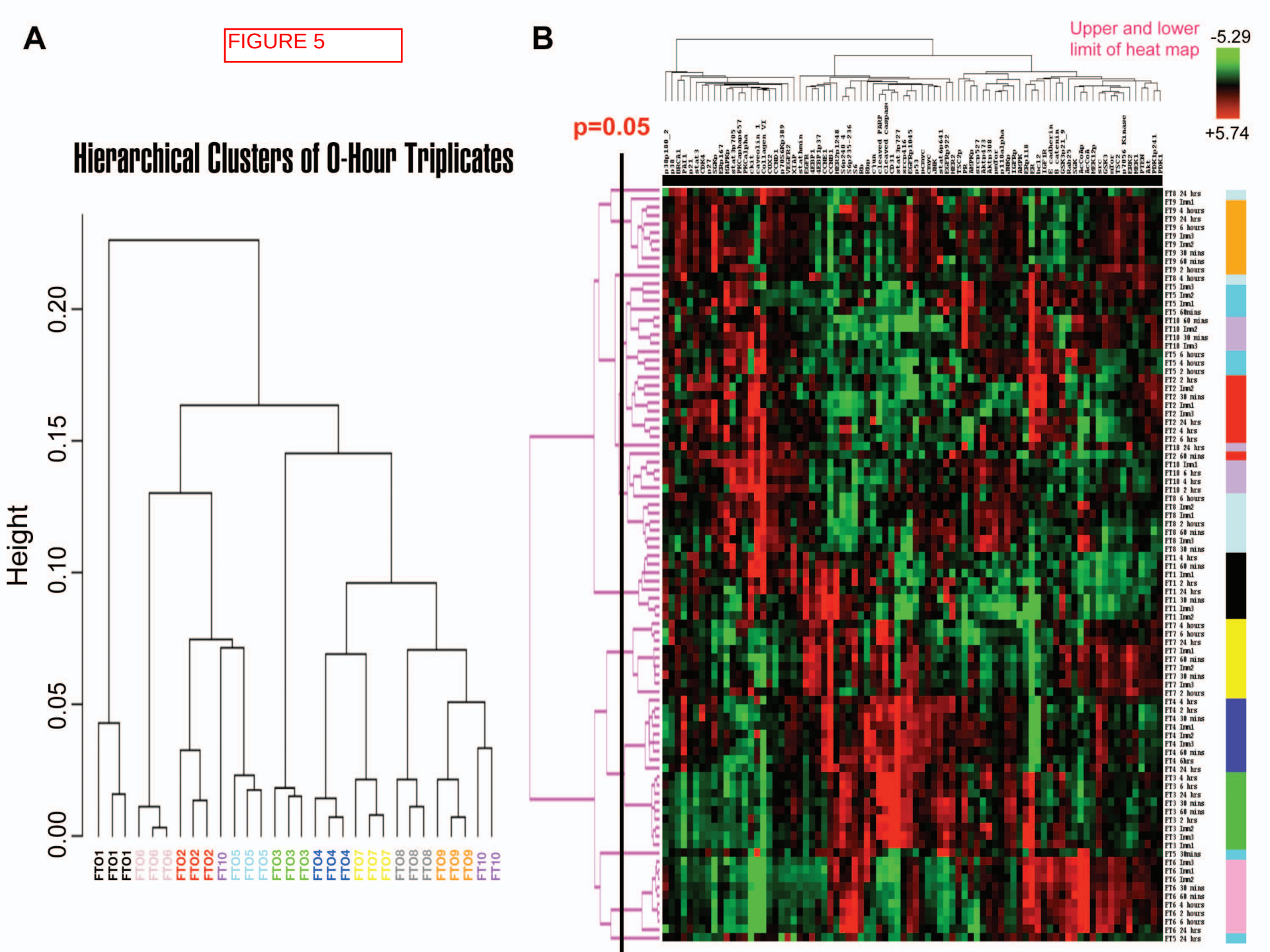
A
Hierarchical Clusters of 0-Hour Triplicates
Height
0.00
0.05
0.10
0.15
0.20
FT01 FT01 FT01 FT06 FT06 FT06 FT02 FT02 FT02 FT10 FT05 FT05 FT05 FT03 FT03 FT03 FT04 FT04 FT04 FT07 FT07 FT07 FT08 FT08 FT08 FT09 FT09 FT09 FT10 FT10
B
Upper and lower limit of heat map
-5.29
+5.74
p=0.05

FIGURE 1-SUPP

Reproducibility experiment

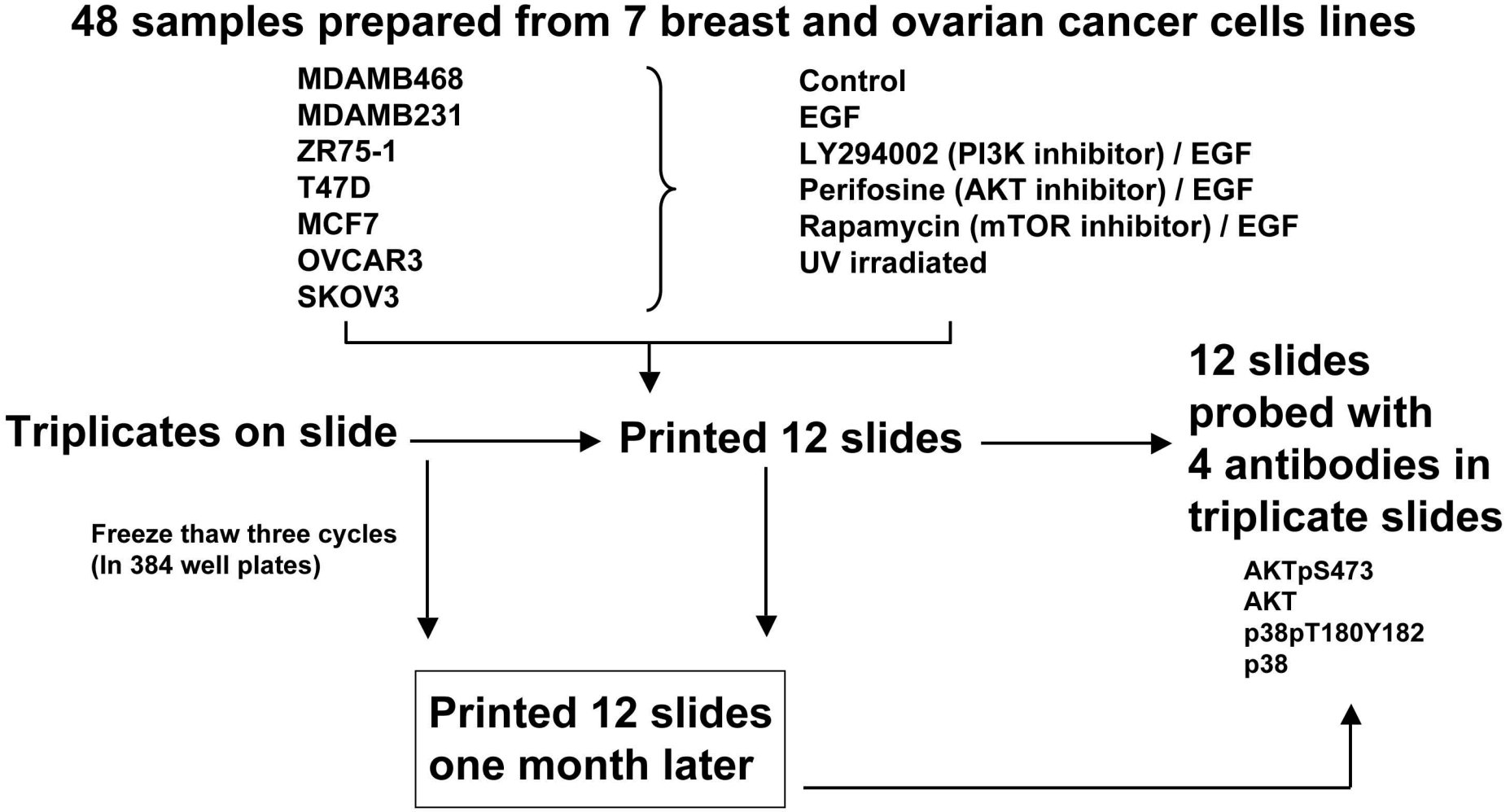

FIGURE 2-SUPP

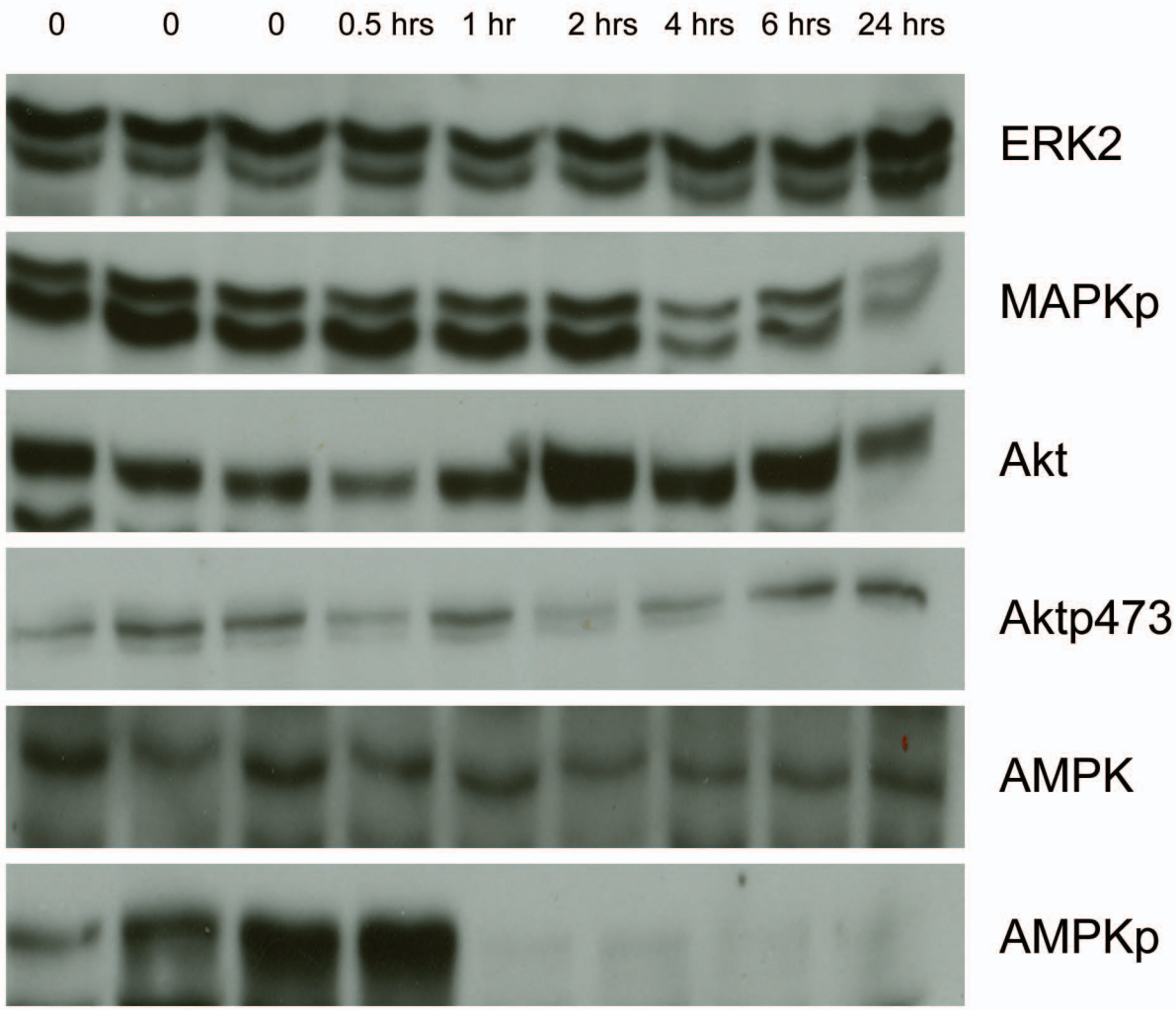

FIGURE 3-SUPP